Joachim Brossmann, MD • Axel Stäbler, MD • Klaus W. Preidler, MD
Debra Trudell, RA • Donald Resnick, MD

Sternoclavicular Joint: MR Imaging–Anatomic Correlation[1]

PURPOSE: **To correlate magnetic resonance (MR) images of the sternoclavicular joint with anatomic sections.**

MATERIALS AND METHODS: **MR imaging was performed on 14 sternoclavicular joints in seven specimens from cadavers (three men and four women 64–94 years of age at death; mean, 84 years). MR arthrography was performed in four specimens (eight joints), after injection of gadopentetate dimeglumine. After imaging, the specimens were frozen and cut into 3-mm-thick slices along the MR imaging planes. Images were correlated with the anatomic slices.**

RESULTS: **MR imaging depicted the anatomy of the sternoclavicular joint and surrounding soft tissue. T2-weighted and proton-density–weighted images were superior to T1-weighted images in depiction of the intraarticular disk. MR arthrography depicted best the intraarticular disk and four of five perforations and delineated the joint capsule. All perforations also were depicted on T2-weighted images.**

CONCLUSION: **MR imaging allows delineation of all structures of the sternoclavicular joint. MR arthrography allows delineation of perforations of the intraarticular disk.**

Index terms: Joints, MR, 473.121411, 473.122 • Joints, sternoclavicular, 473.121411, 473.122, 473.92

Radiology 1996; 198:193–198

THE sternoclavicular joint is the only articulation that joins the upper extremity and the torso. Despite the wide range of motion and the great range of forces on this joint, abnormalities of the sternoclavicular joint are rare, and only infrequently is it injured in sports and accidents. The sternoclavicular joint can be affected, however, by numerous diseases and infections (1–5). Assessment of dislocation in a patient who has sustained trauma is another important indication for imaging of the sternoclavicular joints (6,7).

Plain radiography and conventional tomography are helpful in the diagnosis of most of these abnormalities, but because of superimposed structures, computed tomographic (CT) techniques are preferred, especially in injured patients (7–9). Studies have suggested use of magnetic resonance (MR) imaging in the evaluation of disorders of the sternoclavicular joint (10,11). The purpose of our study was to evaluate the use of MR imaging in examination of structures in the sternoclavicular joint and surrounding ligaments.

ANATOMIC CONSIDERATIONS

The sternoclavicular joint is a diarthrodial saddle joint bounded by the bulbous medial end of the clavicle, the concave saddle-shaped clavicular notch of the manubrium sterni, and the cartilaginous part of the first rib (Fig 1). The articular surface of the clavicle is covered by fibrocartilage thicker than that which covers the articular surface of the sternum. Owing to a discrepancy in size between the two articular surfaces, the stability of the sternoclavicular joint depends primarily on surrounding ligaments.

The fibrocartilaginous intraarticular disk is flat and nearly circular. It lies between the articular surfaces of the clavicle and the manubrium sterni, dividing the joint into two synovium-lined cavities (Fig 1). The two joint cavities differ in size: the inferomedial cavity is smaller than the superolateral cavity. The intraarticular disk originates from the junction between the first costal cartilage and the sternum and inserts on the posterosuperior surface of the medial edge of the clavicle (Fig 1). In the anterior and posterior aspects the disk is attached to the fibrous capsule.

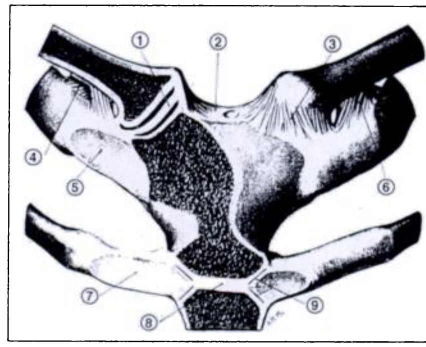

Figure 1. Anterior aspect of the sternoclavicular joint. The right sternoclavicular joint is cut in the coronal plane. *1* = intraarticular disk, *2* = interclavicular ligament, *3* = anterior sternoclavicular ligament, *4* = costoclavicular ligament, posterior fibers, *5* = first costal cartilage, *6* = costoclavicular ligament (anterior fibers), *7* = second costal cartilage, *8* = manubriosternal joint, *9* = second sternocostal joint. (Adapted, with permission, from reference 12.)

The anterior and posterior sternoclavicular ligaments reinforce the fibrous joint capsule (12). The anterior sternoclavicular ligament is presumed to be the strongest ligament of the sternoclavicular joint (13). It is attached to the anterosuperior aspect of the medial epiphysis of the clavicle, to which it is mediocaudal, and inserts on the ventral surface on the upper part of the manubrium sterni.

The posterior sternoclavicular ligament attaches to the posterior surface

Abbreviation: FOV = field of view.

[1] From the Department of Radiology, Veterans Administration Medical Center, 3350 La Jolla Village Dr, San Diego, CA 92161. From the 1995 RSNA scientific assembly. Received May 15, 1995; revision requested June 20; revision received July 10; accepted July 14. Supported in part by Veterans Administration grant SA360 and Deutsche Forschungsgemeinschaft grant BR 149911-1. **Address reprint requests to** D.R.

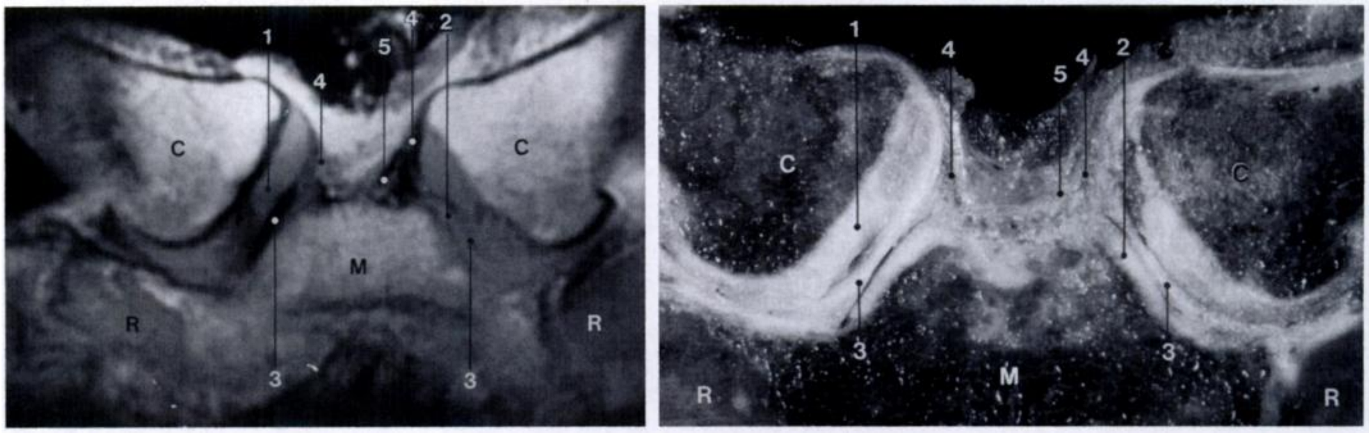

a. b.

Figure 2. Coronal sections through the sternoclavicular joint of an 80-year-old man. **(a)** T1-weighted spin-echo MR image (500/20, 256 × 192 matrix, 14-cm FOV, two signals acquired). **(b)** Corresponding anatomic slice. *C* = clavicle, *M* = manubrium sterni, *R* = first rib, *1* = articular cartilage of clavicle, *2* = articular cartilage of manubrium, *3* = intraarticular disk, *4* = capsule, *5* = interclavicular ligament (fibers).

of the medial aspect of the clavicle but is less distinct than the anterior sternoclavicular ligament. The posterior sternoclavicular ligament is mediocaudal to the clavicle; the insertion is on the dorsal surface of the superior aspect of the manubrium.

The interclavicular ligament is a tough band of fibers that connects the clavicles in the superior and medial aspects (Fig 1). The costoclavicular ligament is attached to the undersurface of the medial clavicle and to the superior rim of the first rib and costal cartilage (Fig 1). Two different fasciculi exist within this ligament: an anterior fasciculus, which is directed craniolaterally, and a posterior fasciculus, which is oriented in the craniomedial direction (12).

Several muscles have origins or insertions on the medial end of the clavicle. The origin of part of the sternocleidomastoid muscle is on the medial half of the superior surface of the clavicle. The insertion of some fibers of the pectoralis major muscle is on the medial anterior surface of the clavicle. The origin of part of the sternohyoid muscle is dorsal to the attachment of the costoclavicular ligament on the inferior surface of the clavicle. The subclavius muscle, which connects the first rib and the clavicle, is attached by a thick tendon to the first costal cartilage anterior to the costoclavicular ligament. Laterally, it is attached to the undersurface of the middle third of the clavicle.

MATERIALS AND METHODS

Fourteen fresh sternoclavicular joints from seven human cadavers (three men and four women 64–94 years of age at the time of death; mean age, 84 years) were examined. Images were obtained with a 1.5-T MR unit (Signa; GE Medical Systems, Milwaukee, Wis) with a circular 5-inch (12.7 cm) receive surface coil. The specimens were placed anterior surface down on the coil, which was centered on the superior sternal notch.

Imaging parameters included spin-echo pulse sequences with repetition times of 500 msec and 2,000 msec and echo times of 20 msec and 80 msec (repetition time msec/echo time msec = 500/20 and 2,000/20, 80). The field of view (FOV) was 14 cm in all examinations. The data-acquisition matrix was 256 × 192 for the T1-weighted images and 256 × 128 for the T2-weighted and proton-density–weighted images. A section thickness of 3 mm was used with a 1-mm intersection gap. Two signals were acquired. Imaging was performed in the transaxial, sagittal, and coronal planes and in an oblique plane along the long axis of the clavicle.

After completion of MR imaging, MR arthrography was performed on the sternoclavicular joints of four specimens (eight joints). A 2-mmol solution of gadopentetate dimeglumine (1 mL of Magnevist [Schering, Berlin, Germany] diluted in 250 mL of saline solution) was injected into the joints with a 23-gauge needle under fluoroscopic guidance. Images of these four specimens were obtained with T1-weighted and fat-suppressed T1-weighted spin-echo sequences.

After imaging, the specimens were deep-frozen for 24 hours (Forma Bio-Freezer; Forma Scientific, Marietta, Ohio). Then, each specimen was cut with a band saw into 3-mm slices along one of the imaging planes. Each slice was examined and photographed for correlation with MR appearance. Correlation was based on the subjective impressions of the authors (J.B., A.S.).

RESULTS

The anatomy of the sternoclavicular joint was demonstrated best with T1-weighted spin-echo MR images. These images depicted all ligaments and soft tissue around the sternoclavicular joint. The fibrous capsule, posterior sternoclavicular ligament, and anterior sternoclavicular ligament were of low signal intensity in all imaging sequences and imaging planes.

On T1-weighted images, the intraarticular disk was depicted as an area of low to intermediate signal intensity. Calcified intraarticular disks appeared as areas of lower signal intensity on T1-weighted images, and they were easier to visualize than noncalcified disks. At macroscopic inspection of the sliced specimens, calcification of the intraarticular disk appeared as localized white areas within the disk. Calcification was present in four of seven specimens.

Differentiation of the fibrocartilaginous intraarticular disk from the articular surface was easier on T2-weighted and proton-density–weighted images than on T1-weighted images. On T2-weighted images, the intraarticular disk appeared as an area of low signal intensity surrounded by areas of high signal intensity, which represented the joint space and articular cartilage. On proton-density–weighted images, the intraarticular disk appeared as an area of low signal intensity, but the articular cartilage and joint space were not delineated as well as they were on T2-weighted images. Although an increase in signal intensity of the intraarticular disk on T2-weighted and proton-density–weighted images suggested abnormality of the disk, the type of abnormality was confirmed only with MR arthrography. No definite alterations in intradiskal signal intensity were found on T1-weighted images. Five of 14 sternoclavicular joints showed alterations in signal intensity consistent

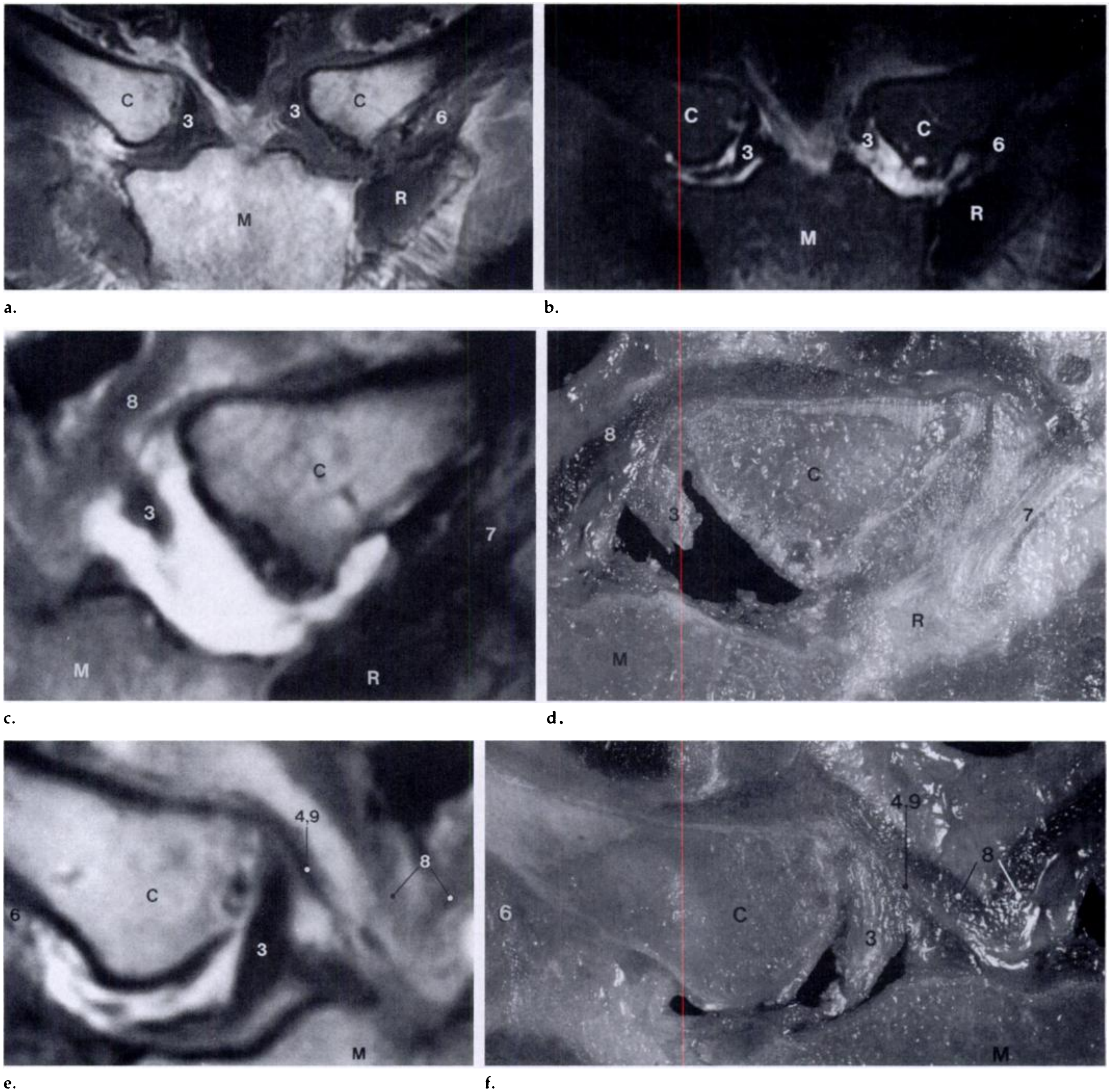

Figure 3. Coronal sections through the sternoclavicular joint of a 92-year-old woman. **(a)** T1-weighted spin-echo MR image (500/20, 256 × 192 matrix, 14-cm FOV, two signals acquired). **(b)** T2-weighted spin-echo MR image (2,000/80, 256 × 128 matrix, 14-cm FOV, two signals acquired). Small amounts of synovial fluid allow delineation of disk perforation on the left side and possible perforation on the right. **(c)** T1-weighted spin-echo MR arthrogram (500/20, 256 × 192 matrix, 14-cm FOV, two signals acquired) of the left sternoclavicular joint shows disk perforation. **(d)** Corresponding anatomic slice. **(e)** T1-weighted spin-echo MR arthrogram (500/20, 256 × 192 matrix, 14-cm FOV, two signals acquired) of right sternoclavicular joint shows no disk perforation. **(f)** Corresponding anatomic slice. *C* = clavicle, *M* = manubrium sterni, *R* = first rib, *3* = intraarticular disk, *4* = capsule, *6* = costoclavicular ligament, *7* = subclavius muscle, insertion of tendon at first rib, *8* = sternocleidomastoid muscle, *9* = anterior sternoclavicular ligament.

with perforation of the disk. The presence of four perforations was confirmed with MR arthrography.

Coronal Plane

Imaging in the coronal imaging plane (Figs 2, 3) was best suited for displaying the articular surfaces of the medial end of the clavicle and the manubrium. The coronal imaging plane also was best for delineating the entire intraarticular disk and for demonstrating perforations. The disk usually was thicker in its periphery, especially the posterosuperior part. The origin of the disk near the junction between the first costal cartilage and the sternum and the insertion of the disk on the medial edge of the posterosuperior surface of the clavicle were demonstrated.

In the medial aspect, the joint capsule could not be differentiated from the fibers of the interclavicular ligament. At its lateral attachment at the undersurface of the clavicle, the joint capsule was not well demonstrated. MR arthrography helped delineate the extent of the capsule.

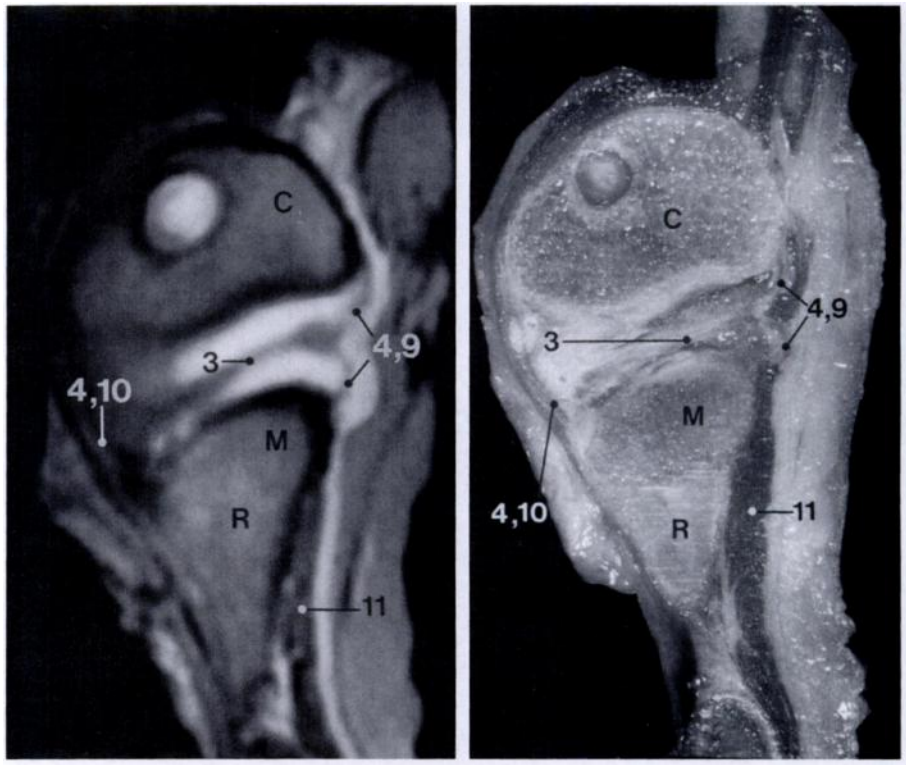

a. b.

Figure 4. Sagittal sections through the sternoclavicular joint in a 64-year-old woman. **(a)** T1-weighted spin-echo MR arthrogram (500/20, 256 × 192 matrix, 14-cm FOV, two signals acquired) demonstrates both joint cavities and attachment of the disk to the joint capsule. **(b)** Corresponding anatomic slice. A subchondral cyst communicates with the joint space. *C* = clavicle, *M* = manubrium sterni, *R* = first rib, *3* = intraarticular disk, *4* = capsule, *9* = anterior sternoclavicular ligament, *10* = posterior sternoclavicular ligament, *11* = pectoralis muscle. Anterior surface faces the right.

The anterior and posterior sternoclavicular ligaments were not well demonstrated in the coronal plane. The costoclavicular ligament was well delineated, but differentiation between anterior and posterior portions was not possible. Anterior to the costoclavicular ligament, the tendon of the subclavius muscle was evident, as was the insertion of the muscle on the first costal cartilage. The lateral insertion of the muscle on the undersurface of the middle third of the clavicle also was delineated.

Sagittal Plane

Use of the sagittal imaging plane (Figs 4,5) allowed the best delineation of the anteroposterior thickness of the costoclavicular ligament. The two fasciculi of this ligament and the bursa between the fasciculi were not differentiated, however. Sagittal images also showed the position of the subclavius muscle, which was under the clavicle and anterior to the costoclavicular ligament. The extent of the anterior and posterior sternoclavicular ligaments was defined, and the attachment of the intraarticular disk anterior and posterior to the joint capsule was seen. Although the disk and the two joint cavities were seen on images in this plane, diagnosis of disk perforations was not possible with routine MR imaging.

Transaxial Plane

Use of the transaxial imaging plane (Fig 6) allowed depiction of the anterior and posterior parts of the joint capsule and the anterior and posterior sternoclavicular ligaments. Single images viewed in this plane, however, did not demonstrate optimally the position of the clavicles in relation to the manubrium. The anterior and posterior attachments of the intraarticular disk to the joint capsule were depicted. Delineation of perforations of the intraarticular disk was not possible. Use of the transaxial plane also

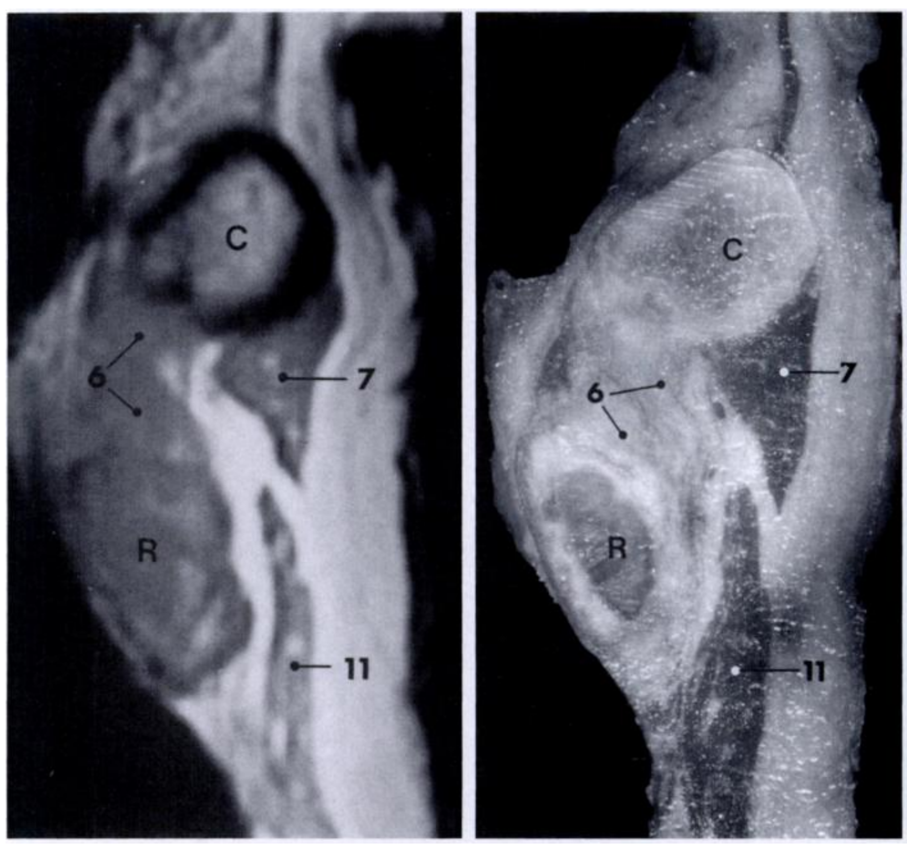

a. b.

Figure 5. Sagittal sections through area of the interclavicular ligament in a 64-year-old woman. **(a)** T1-weighted spin-echo MR image (500/20, 256 × 192 matrix, 14-cm FOV, two signals acquired). **(b)** Corresponding anatomic slice. *C* = clavicle, *R* = first rib, *6* = costoclavicular ligament, *7* = subclavius muscle, *11* = pectoralis muscle. Anterior surface faces the right.

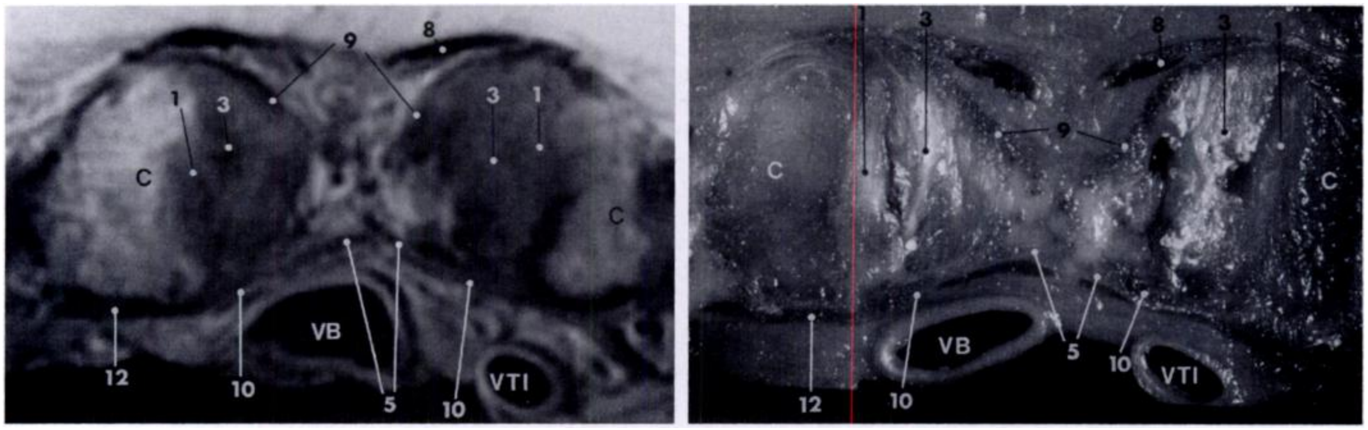

a. b.

Figure 6. Transaxial sections through the sternoclavicular joint of an 86-year-old woman. **(a)** T1-weighted spin-echo MR image (500/20, 256 × 192 matrix, 14-cm FOV, two signals acquired). **(b)** Corresponding anatomic slice. *C* = clavicle, *VB* = brachiocephalic vein, *VTI* = inferior thyroid vein, *1* = articular cartilage of the clavicle, *3* = intraarticular disk, *5* = interclavicular ligament, *8* = sternocleidomastoid muscle, *9* = anterior sternoclavicular ligament, *10* = posterior sternoclavicular ligament, *12* = sternothyroid muscle. Anterior surface faces the top.

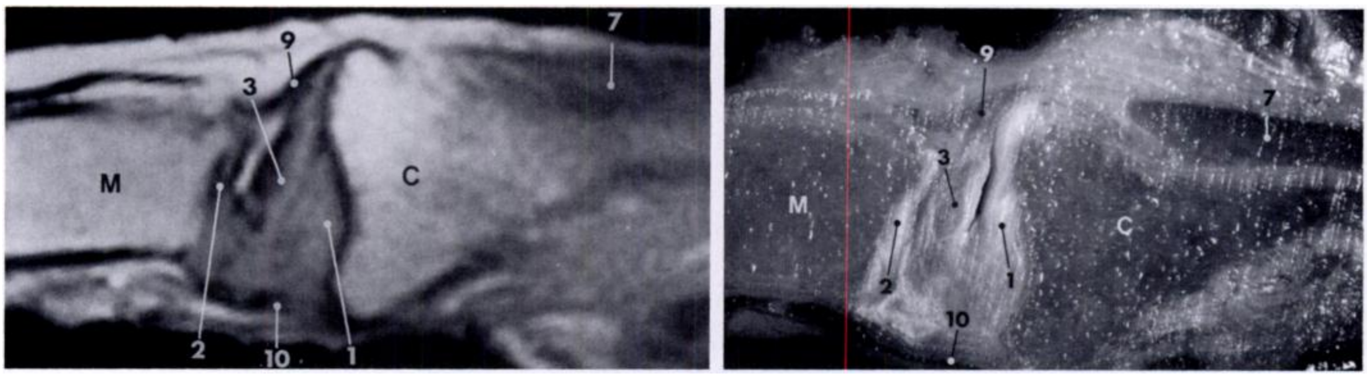

a. b.

Figure 7. Oblique sections parallel to the long axis of the clavicle in a 67-year-old woman. **(a)** T1-weighted spin-echo MR image (500/20, 256 × 192 matrix, 14-cm FOV, two signals acquired). **(b)** Corresponding anatomic slice. *C* = clavicle, *M* = manubrium sterni, *1* = articular cartilage of the clavicle, *2* = articular cartilage of manubrium, *3* = intraarticular disk, *7* = subclavius muscle, *9* = anterior sternoclavicular ligament, *10* = posterior sternoclavicular ligament.

allowed demonstration of the costoclavicular and the interclavicular ligaments. The close relation between the sternoclavicular joint and the great vessels and trachea was shown.

Oblique Transaxial Plane

Use of the oblique transaxial plane (Fig 7) allowed the best assessment of the relation of the medial end of the clavicle to the manubrium. The extent and course of the anterior and posterior sternoclavicular ligaments were depicted in great detail. The posterosuperior attachment of the intraarticular disk to the medial end of the clavicle also was well demonstrated.

DISCUSSION

Several diseases involve the sternoclavicular joint. It can be a site of location for infection, especially in drug users (1,4,5,14,15). The sternoclavicular joint also may be affected in patients with seronegative spondyloarthropathies (3), rheumatoid arthritis (16), and hyperparathyroidism (17,18). The sternoclavicular joints are a typical site of involvement in the SAPHO syndrome (synovitis, acne, pustulosis, hyperostosis, osteitis), which comprises chronic recurrent multifocal osteomyelitis (CRMO), osteitis condensans of the clavicle, sternocostoclavicular hyperostosis, and various forms of pustulotic arthro-osteitis (2,9,11,19–21). Degenerative changes in the sternoclavicular joint affect the clavicle and the fibrocartilaginous disk (22). Perforations of the disk and chondrocalcinosis with deposition of calcium pyrophosphate dihydrate are common (22,23). Dislocation of the clavicle (6,7) is associated with injuries to the anterior and posterior sternoclavicular ligaments. With additional superior displacement of the clavicle, the costoclavicular ligament also is disrupted.

Radiographs of the sternoclavicular joints often are inadequate. Standard projections include posteroanterior, oblique, and lateral views, although these projections often do not display the sternoclavicular joint adequately. Special radiographic projections of the sternoclavicular joint have been described (24–26), but they are used primarily to demonstrate dislocations of the joint. For better visualization of the joint surfaces and subtle intraosseous changes, conventional tomography or CT has been used (14,15,20). To our knowledge, the role of MR imaging in the diagnosis of sternoclavicular joint diseases has not been defined, although a few descriptions of the use of MR imaging in the assessment of disorders of the sternoclavicular joint do exist (10,11,21).

Our results, derived from close correlation of MR images and anatomic slices, suggest that the anatomy of the sternoclavicular joint and the surrounding tissues can be demonstrated in detail. All the ligaments around the sternoclavicular joint can be delineated with conventional MR imaging sequences. The anterior and posterior sternoclavicular joints can be partially demonstrated on coronal images, can be well demonstrated on transaxial and sagittal images, and can be best demonstrated on oblique images, which parallel the long axis of the clavicle. The interclavicular ligament can be evaluated best on coronal images, although it also can be seen on transaxial and sagittal images. The coronal and sagittal planes appear most favorable for imaging the costoclavicular ligament.

The intraarticular disk is best demonstrated in its entirety in the coronal plane. This disk is difficult to differentiate from the fibrocartilaginous articular surfaces on T1-weighted images unless it is calcified. Although it is well demonstrated on conventional MR images with T2-weighted and proton-density–weighted imaging sequences, the disk is best delineated with MR arthrography combined with T1-weighted or T1-weighted fat-saturated imaging. MR arthrography demonstrated perforations of the intraarticular disk in four of five sternoclavicular joints in which perforations were present. Although this is a high prevalence of perforation, it is known that this type of lesion is common in elderly people (22). The clinical relevance of this finding is unclear and probably is unimportant. MR arthrography also allows evaluation of the boundaries of the joint capsule.

These results are promising with regard to the potential of MR imaging in assessment of traumatic and nontraumatic disorders about the sternoclavicular joint. The images were obtained in cadavers, however, so motion artifacts were eliminated. In patients, these studies are likely to be limited by respiratory motion artifact, although faster imaging sequences and developments in gating techniques should make MR imaging of the sternoclavicular joint feasible. The ability of MR imaging to allow direct assessment of supporting structures around the joint and the cartilaginous epiphysis may prove useful in the assessment of injuries to the sternoclavicular joint (27,28). ■

References

1. Karten I. Septic arthritis complicating rheumatoid arthritis. Ann Intern Med 1969; 70:1147–1158.
2. Kahn MF, Chamot AM. SAPHO syndrome. Rheum Dis Clin North Am 1992; 18:225–246.
3. Jurik AG. Anterior chest wall involvement in seronegative arthritides: a study of frequencies of changes at radiography. Rheumatol Int 1992; 12:7–11.
4. Berrocal A, Gotuzzo E, Calvo A, et al. Sternoclavicular brucellar arthritis: a report of 7 cases and a review of literature. J Rheumatol 1993; 20:1184–1186.
5. Reginato AJ. Syphilitic arthritis and osteitis. Rheum Dis Clin North Am 1993; 19: 379–398.
6. Nettles JL, Linscheid R. Sternoclavicular dislocations. J Trauma 1968; 8:158–164.
7. Cope R. Dislocations of the sternoclavicular joint. Skeletal Radiol 1993; 22:233–238.
8. Hatfield MK, Gross BH, Glazer GM, et al. Computed tomography of the sternum and its articulations. Skeletal Radiol 1984; 11: 197–203.
9. Greenspan A, Gerscovich E, Szabo RM, et al. Condensing osteitis of the clavicle: a rare but frequently misdiagnosed condition. AJR 1991; 156:1011–1015.
10. Shanley DJ, Vassallo CJ, Buckner AB. Sternoclavicular pyarthrosis demonstrated on bone scan: correlation with CT and MRI. Clin Nucl Med 1991; 16:786–787.
11. Vierboom MAC, Steinberg JDJ, Mooyaart EL, et al. Condensing osteitis of the clavicle: magnetic resonance imaging as an adjunct method for differential diagnosis. Ann Rheum Dis 1992; 51:539–541.
12. Williams PC, Warwick R, eds. Anatomy of the human body. 37th ed. New York, NY: Churchill Livingstone, 1989.
13. Bearn JG. Direct observations on the function of the capsule of the sternoclavicular joint in clavicular support. J Anat 1967; 101:159–170.
14. Covelli M, Lapadula G, Pipitone N, et al. Isolated sternoclavicular joint arthritis in heroin addicts and/or HIV positive patients: three cases. Clin Rheumatol 1993; 12:422–425.
15. Van Linthoudt D, Velan F, Ott H. Abscess formation in sternoclavicular joint septic arthritis. J Rheumatol 1989; 16:413–414.
16. Kalliomaki JL, Viitanen S-M, Virtama P. Radiological findings of sternoclavicular joints in rheumatoid arthritis. Acta Rheumatol Scand 1968; 14:233–240.
17. Teplick JG, Eftekhari F, Haskin ME. Erosion of the sternal ends of the clavicles: a new sign of primary and secondary hyperparathyroidism. Radiology 1974; 113:323–326.
18. Resnick D, Niwayama G. Subchondral resorption of bone in renal osteodystrophy. Radiology 1976; 118:315–321.
19. Köhler H, Uehlinger E, Kutzner J, et al. Sternocostoclavicular hyperostosis: painful swelling of the sternum, clavicles, and upper ribs: report of two new cases. Ann Intern Med 1977; 87:192–197.
20. Chigira M, Shimizu T. Computed tomographic appearances of sternoclavicular hyperostosis. Skeletal Radiol 1989; 18:347–352.
21. Ginalski JM, Landry M, Rappoport G, et al. MR imaging of sternocostoclavicular arthro-osteitis with palmoplantar pustulosis. Eur J Radiol 1992; 14:221–222.
22. Kier R, Wain SL, Apple J, et al. Osteoarthritis of the sternoclavicular joint: radiographic features and pathologic correlation. Invest Radiol 1986; 21:227–233.
23. Resnick D, Niwayama G, Goergen TG, et al. Clinical, radiographic and pathologic abnormalities in calcium pyrophosphate dihydrate deposition disease (CPPD): pseudogout. Radiology 1977; 122:1–15.
24. Kurzbauer R. The lateral projection in roentgenography of the sternoclavicular articulation. AJR 1946; 56:104–105.
25. Heinig CF. Retrosternal dislocation of the clavicle: early recognition, x-ray diagnosis and management (abstr). J Bone Joint Surg [Am] 1968; 50:830.
26. Hobbs DW. Sternoclavicular joint: a new axial radiographic view. Radiology 1968; 90:801.
27. Brooks AL, Henning GD. Injury to the proximal clavicular epiphysis. J Bone Joint Surg [Am] 1972; 54:1347–1348.
28. Jaramillo D, Hoffer FA. Cartilaginous epiphysis and growth plate: normal and abnormal MR imaging findings. Radiology 1992; 158:1105–1110.